

12-15-2002

Feline Immunodeficiency Virus Integration in B-Cell Lymphoma Identifies a Candidate Tumor Suppressor Gene on Human Chromosome 15q151

Julia Beatty
University of Glasgow

Anne Terry
University of Glasgow


Julie MacDonald
University of Glasgow

Elizabeth Gault
University of Glasgow

Stanley Cevario
National Cancer Institute at Frederick

See next page for additional authors

Follow this and additional works at: https://nsuworks.nova.edu/cnso_bio_facarticles

 Part of the [Genetics and Genomics Commons](#), and the [Medicine and Health Sciences Commons](#)

NSUWorks Citation

Beatty, Julia; Anne Terry; Julie MacDonald; Elizabeth Gault; Stanley Cevario; Stephen J. O'Brien; Ewan Cameron; and James C. Neil. 2002. "Feline Immunodeficiency Virus Integration in B-Cell Lymphoma Identifies a Candidate Tumor Suppressor Gene on Human Chromosome 15q151." *Cancer Research* 62, (24): 7175-7180. https://nsuworks.nova.edu/cnso_bio_facarticles/670

This Article is brought to you for free and open access by the Department of Biological Sciences at NSUWorks. It has been accepted for inclusion in Biology Faculty Articles by an authorized administrator of NSUWorks. For more information, please contact nsuworks@nova.edu.

Authors

Julia Beatty, Anne Terry, Julie MacDonald, Elizabeth Gault, Stanley Cevario, Stephen J. O'Brien, Ewan Cameron, and James C. Neil

Feline Immunodeficiency Virus Integration in B-Cell Lymphoma Identifies a Candidate Tumor Suppressor Gene on Human Chromosome 15q15¹

Julia Beatty,^{2,3} Anne Terry,³ Julie MacDonald, Elizabeth Gault, Stan Cevario, Stephen J. O'Brien, Ewan Cameron, and James C. Neil⁴

Molecular Oncology Laboratory, Institute of Comparative Medicine, University of Glasgow Veterinary School, Bearsden, Glasgow, Scotland G61 1QH [J. B., A. T., J. M., E. G., E. C., J. C. N.], and Laboratory of Genomic Diversity, National Cancer Institute, Frederick, Maryland 21702 [S. C., S. J. O.]

Abstract

Infection with immunosuppressive lentiviruses is associated with increased cancer risk, but most studies have implicated indirect mechanisms as the tumor cells generally lack integrated viral sequences. An exception was found in a B-cell lymphoma (Q254) where the tumor cells contained a single integrated feline immunodeficiency virus genome. Additional analysis now indicates that feline immunodeficiency virus integration in lymphoma Q254 resulted in promoter insertion and truncation of a conserved gene on feline chromosome B3, whereas the unaffected allele of the gene appeared to be transcriptionally down-regulated. The orthologous human gene (*FLJ12973*), is expressed ubiquitously and encodes a WD-repeat protein with structural similarity to DDB2, the small subunit of the xeroderma pigmentosum XP-E complex. Moreover, the gene is located within a region of frequent tumor-specific deletions on chromosome 15q15. These observations demonstrate the direct mutagenic potential of the lentiviruses and identify a new candidate tumor suppressor gene.

Introduction

Retrovirus-induced cancers frequently involve *cis*-activation of host cell oncogenes at the sites of proviral insertion (1). Tumor suppressor gene inactivation is a rarer consequence, but several notable examples include the *p53* gene, where biallelic retroviral inactivation provided an early clue to its tumor suppressor status (2). However, the importance of insertional mutagenesis as a carcinogenic mechanism has been established only for the simple α , β , and γ retroviruses. Tumors associated with HIV and related lentiviruses have generally been found to lack viral sequences, suggesting that the tumor predisposition conferred by this subfamily of retroviruses is because of indirect mechanisms. Most HIV-1-associated lymphomas are thought to occur secondary to polyclonal B-cell activation and infection with oncogenic viral cofactors such as EBV or HHV-8 (3). Similarly, longitudinal monitoring of cats infected with FIV⁵ has documented impaired cell-mediated immunity and B-cell hyperactivity as factors that may contribute indirectly to lymphomagenesis (4), whereas analyses of a series of FIV-associated lymphomas showed that most of these lacked detectable viral sequences (5). Despite these generally negative observations, a number of studies have suggested

that there may be exceptions to this rule. HIV sequences have been detected in a number of tumors using PCR methods (6, 7). Moreover, monoclonal integration of viral sequences in the tumor DNA was demonstrated for one case of HIV-associated T-cell lymphoma where viral integration was mapped to the *FUR* gene and was associated with overexpression of the nearby *FPS/FES* proto-oncogene (8). We reported a potentially similar observation in a case of B-cell lymphoma, which arose in a cat infected with FIV, where the tumor cells harbored a single integrated proviral copy detected by Southern blot analysis (9). Additional analysis reported here suggests that in this case the consequence of this insertion event may be loss of function rather than transcriptional activation of a host gene. Furthermore, analysis of the human orthologue reveals a previously uncharacterized gene, which maps to a site of frequent deletions and loss of heterozygosity in a number of common human cancers.

Materials and Methods

Library Preparation and Screening. DNA extracted from lymphoma Q254 (9) was digested to completion with *EcoRI* and size selected on a 10–40% sucrose gradient. Fragments between 9 and 13 kb were purified, and mixed in a 1:1 molar ratio with *EcoRI* digested λ DASH II arms (Stratagene). After ligation and packaging with Gigapack III Gold extract (Stratagene), $\sim 0.5 \times 10^6$ plaques were screened with a radiolabelled probe generated by random priming of a 1.2 kb FIV Gag-pol fragment (1242–2431; Ref. 10). After plaque purification of positive recombinants, phage DNA was prepared and used for analysis by restriction mapping and Southern blot hybridization. A representative clone was selected for subcloning of the *EcoRI* insert into plasmid pBR328 for additional analysis, generating the plasmid designated pEAG6.

Sequence Analysis. DNA sequence was determined using a Thermosequence primer cycle sequencing kit (Amersham Pharmacia Biotech) with the aid of infrared dye-labeled primers (MWG, Germany) and a LiCor 4000 automated sequencer.

Southern Blot Hybridization. Twenty- μ g samples of DNA were digested with *EcoRI*, fragments separated on a 0.8% agarose TAE gel and transferred onto Hybond N membrane (Amersham Pharmacia Biotech) in 20 \times SSC. The filter was hybridized with a 94-bp exon 3 probe (PCR product of primers C 5'-GATGAATTTTCAGGATTGTC-3' and D 5'-ACCGCAGACAAGTGAAGAG-3', fE3, Fig. 1a) in RapidHyb (Amersham Pharmacia Biotech) at 65°C, washed 3 \times 20 min 0.5 \times SSC, 0.5% SDS, 60°C, and exposed to X-ray film.

Chromosomal Assignment. Chromosomal assignment of the FIV integration site was achieved by PCR screening of feline-rodent hybrid cell lines each containing different combinations of feline chromosomes (11). Primers (A and B) were based on unique feline DNA sequences 5' to the integrated FIV element (Fig. 1, a and c; A: 5'-AGACATAGAAATCTCAAGCAG-3'; B: 5'-ACTTGCTCCTAATTTTACCC-3'), which allowed the amplification of a 250-bp fragment from feline but not hamster or mouse template DNA. One-min steps of denaturation (95°C), annealing (52°C), and DNA synthesis (72°C) were performed using 1 μ g of template DNA, 50 pmol of each primer, and Taq polymerase (Promega Corporation).

Northern Blot Analysis. A human multitissue Northern blot (Clontech) was hybridized in RapidHyb with human EST clone (IMAGE clone 1047426) insert, obtained from the United Kingdom MRC HGMP Resource Centre

Received 5/22/02; accepted 10/31/02.

The costs of publication of this article were defrayed in part by the payment of page charges. This article must therefore be hereby marked *advertisement* in accordance with 18 U.S.C. Section 1734 solely to indicate this fact.

¹ J. B. was supported by the Wellcome Trust United Kingdom. Other aspects of this work were supported by awards from Cancer Research United Kingdom and the Leukemia Research Fund.

² Present address: Sydney Cat Specialists, 70 Roberts St. Camperdown, NSW 2050, Australia.

³ These authors contributed equally to this work.

⁴ To whom requests for reprints should be addressed, at Molecular Oncology Laboratory, Institute of Comparative Medicine, University of Glasgow Veterinary School, Bearsden, Glasgow, Scotland G61 1QH. Phone: 44-141-330-5771; Fax: 44-141-330-4874; E-mail: j.c.neil@vet.gla.ac.uk.

⁵ The abbreviations used are: FIV, feline immunodeficiency virus; EST, expressed sequence tag; RT-PCR, reverse transcription-PCR; HPRT, hypoxanthine phosphoribosyl-transferase; LTR, long terminal repeat.

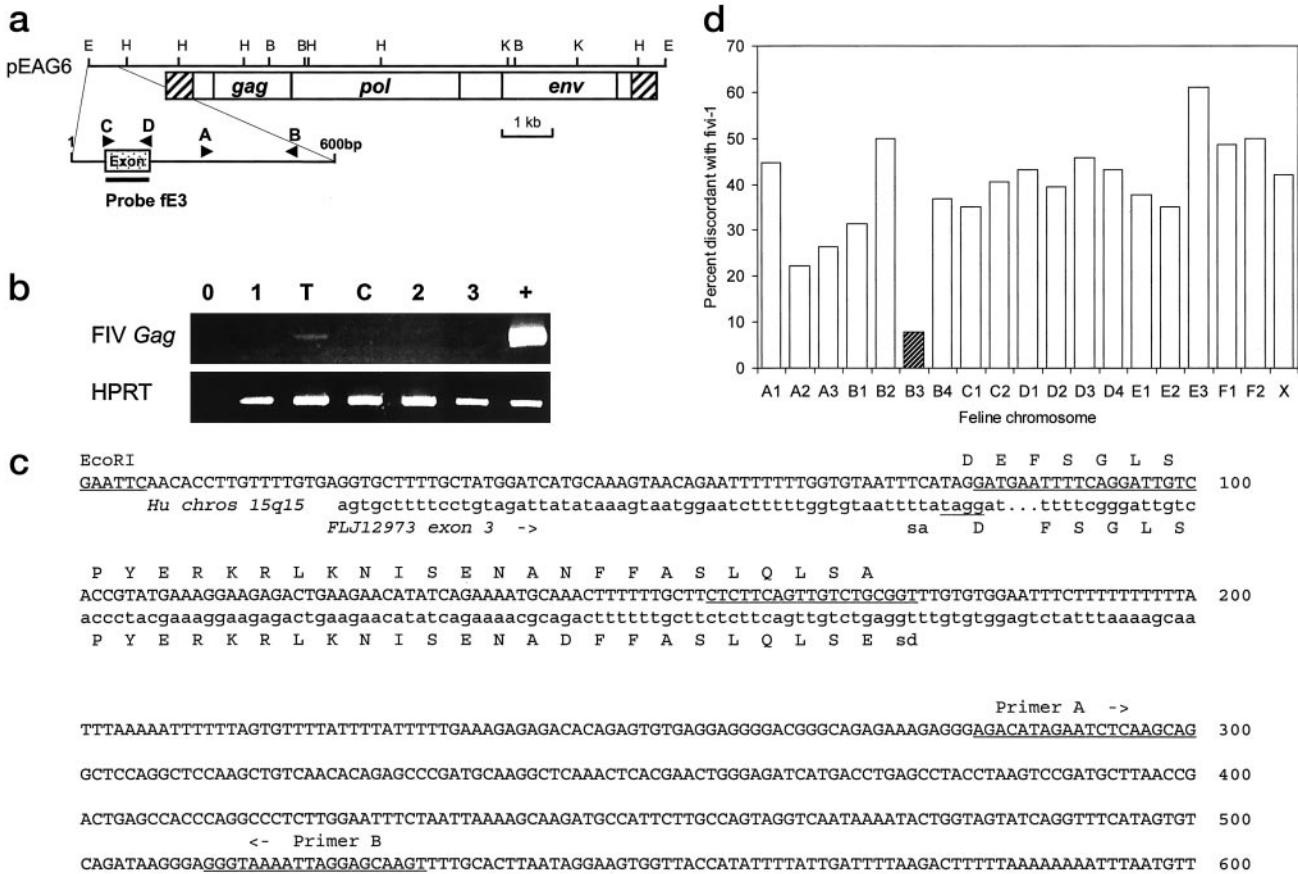


Fig. 1. a, diagram of plasmid pEAG6, containing integrated FIV and host flanking sequences (*FIVi-1*) from lymphoma Q254. The upper lines shows a partial restriction map with sites indicated for *EcoRI* (E), *HindIII* (H), *KpnI* (K), and *BamHI* (B). The expanded line below shows the 5' 600 bp of the insert with the location of a conserved exon (stippled box) and primers used for the chromosomal mapping of the integration site (A and B) and the generation of a unique hybridization probe (C and D, probe fE3). The location of FIV genes is indicated, with \square indicating the LTRs. b, RT-PCR analysis of FIV expression in lymphoma Q254. Primers from the FIV *Gag* gene (966F, 1837R) were used to screen for FIV specific products. The amplification products were separated on a polyacrylamide gel and detected by staining with ethidium bromide. Samples include Q254 lymphoma (T), salivary gland (C). Control samples include no added RNA (0), feline fibroblast RNA (1 and 3), feline lymphoma F422 (2) and the FL4 cell line (+), which is persistently infected with FIV. c, sequence of the 5' 600bp of *EcoRI* clone pEAG6, showing the position and sequence of a conserved exon and its match to the FLJ12973 gene on human chromosome 15. The human DNA sequence is depicted only for the region of match. Primer sequences as defined above are underlined. d, assignment of the FIV integration site *FIVi-1* to feline chromosome B3. DNA from a series of 38 rodent x cat somatic cell hybrid clones was screened for the presence of *FIVi-1* sequences by PCR using primers A and B (a and c). The histogram shows the percentage of discordance between *FIVi-1* and the specified feline chromosomes as defined by 28 established marker genes (11).

(accession number AA625226). Hybridization was carried out at 65°C, and washing was performed at high stringency (3 × 20 min 0.1 × SSC, 0.5% SDS, 60°C).

RT-PCR. Five μg of total RNA samples were reverse transcribed using a First Strand cDNA synthesis kit (Amersham Pharmacia Biotech) and *NorI*-dT primer. Amplification was carried out on aliquots of one-fifth of each sample with 30 pmol of each primer pair. Primers used included F-FLJ12973 exon 3 and 4 (exon 3 5'-AAGGAAGAGACTGAAGAACA-3' and exon 4 5'-TG-GATTCAAGGAGGCTGTCTC-3'), FIV *Gag* (966F 5'-GGGATTAGACAC-TAGGCCATCTA-3', 1837R 5'-GACCAGGTTTCCACATTTATTA-3'), FIV R/U5 (5'-ATTGAACCTGTCAAGTATCT-3'), or HPRT. Amplification was performed in 1.1 × Reddy Mix (ABgene) at 95°C 30 s, 55°C 30 s, and 72°C 30 s. To control for RNA integrity, HPRT amplification was found to require 29 (C), 27 (T), and 25 (0, 1, 2, and 3) cycles (C, T, 0, 1, 2, 3; see Figure legends). Therefore, other primer pairs were normalized to 32 (C), 30 (T), and 28 cycles (0, 1, 2, and 3). Five-μl aliquots of each reaction were separated on 4% polyacrylamide gels, and detected either by staining with ethidium bromide (Fig. 1b; Fig. 3b), or transferred onto Hybond N membrane in 20 × SSC and hybridized in 6 × SSC at 65°C with either fE3 or HPRT probes (Fig. 3d). Washes were 3 × 20 min 0.1 × SSC, 0.5% SDS, 60°C (fE3) or 0.5 × SSC, 0.5% SDS (HPRT).

Results and Discussion

Lymphoma Q254 arose in a specific pathogen-free cat that had been infected with the Glasgow-8 strain of FIV for >6 years. The

tumor was extranodal, high grade, and of immature B-cell origin as demonstrated by immunocytochemical staining and antigen receptor gene analysis. Previous analyses also showed that the tumor DNA contained a single integrated copy of the FIV genome, whereas immunostaining for viral antigen was negative (9).

To characterize the inserted FIV provirus additionally, a bacteriophage library was prepared from high molecular weight Q254 tumor DNA, and this was screened with a FIV-specific *gag-pol* probe. Two positive clones were obtained containing apparently identical *EcoRI* inserts of 11.5 kb, and one of these was analyzed additionally after subcloning into plasmid pBR328 to generate the plasmid clone designated pEAG6. Restriction enzyme mapping and hybridization analysis indicated the presence of an apparently full-length FIV provirus and ~2 kb of host flanking sequence. Sequence analysis confirmed this structure, revealing a full-length FIV genome along with 1770 and 69 bp of cellular flanking sequences from the 5' and 3' ends, respectively (Fig. 1a). The proviral sequence from lymphoma Q254 was found to be very closely related to the original infecting strain (FIV-G8), with an *env* gene match of >98% at the amino acid level (data not shown).

Attempts to recover infectious virus from pEAG6 by a sensitive transfection and coculture method (12) were unsuccessful, suggesting that the tumor-derived viral genome carried a subtle defect that was

not evident from the primary sequence. However, analysis of feline fibroblast cells (CrFK) transfected with pEAG6 showed that FIV structural proteins were expressed at similar levels to a control plasmid carrying an intact infectious molecular clone (data not shown). These observations are interesting in the light of our previous studies, which showed that viral sequences were not detectably expressed in the primary tumor (9). Attempts to resolve these observations by analysis of viral transcription in the primary tumor were severely constrained by lack of primary tumor material, but sufficient RNA was extracted for limited Northern blot and RT-PCR analysis. Whereas Northern blots did not reveal any detectable FIV transcripts (data not shown), a normalized RT-PCR analysis of tumor RNA using FIV-specific primers revealed their presence at low levels (Fig. 1*b*), suggesting that the provirus may have been expressed at low levels. However, the possibility that this signal arose from low levels of tumor-infiltrating lymphoid or myeloid cells could not be excluded.

Analysis of a series of feline-rodent hybrid cell lines was undertaken to assign the FIV integration locus (*FIVi-1*) to a feline chromosome. Primers A and B (Fig. 1, *a* and *c*) were used to amplify a fragment of 250 bp from a panel of 38 cat-rodent hybrids. The lowest level of discordancy was noted with markers on feline chromosome B3, providing an unambiguous assignment to this chromosome (Fig. 1*d*).

Searches for matches to known genes by Basic Local Alignment Search Tool analysis using the flanking sequences revealed a highly significant match to a human gene (*FLJ12973/Q9H967*) that maps to chromosome 15q15. This location is consistent with the presence of an orthologue on feline chromosome B3, which displays syntenic alignment with human chromosomes 14 and 15, and a short region of chromosome 3 (13). The *FLJ12973* gene is highly conserved, as shown by its close homology to its murine orthologue on chromosome 2 (Q9CTV4 at band E5) and by matches to ESTs from other mam-

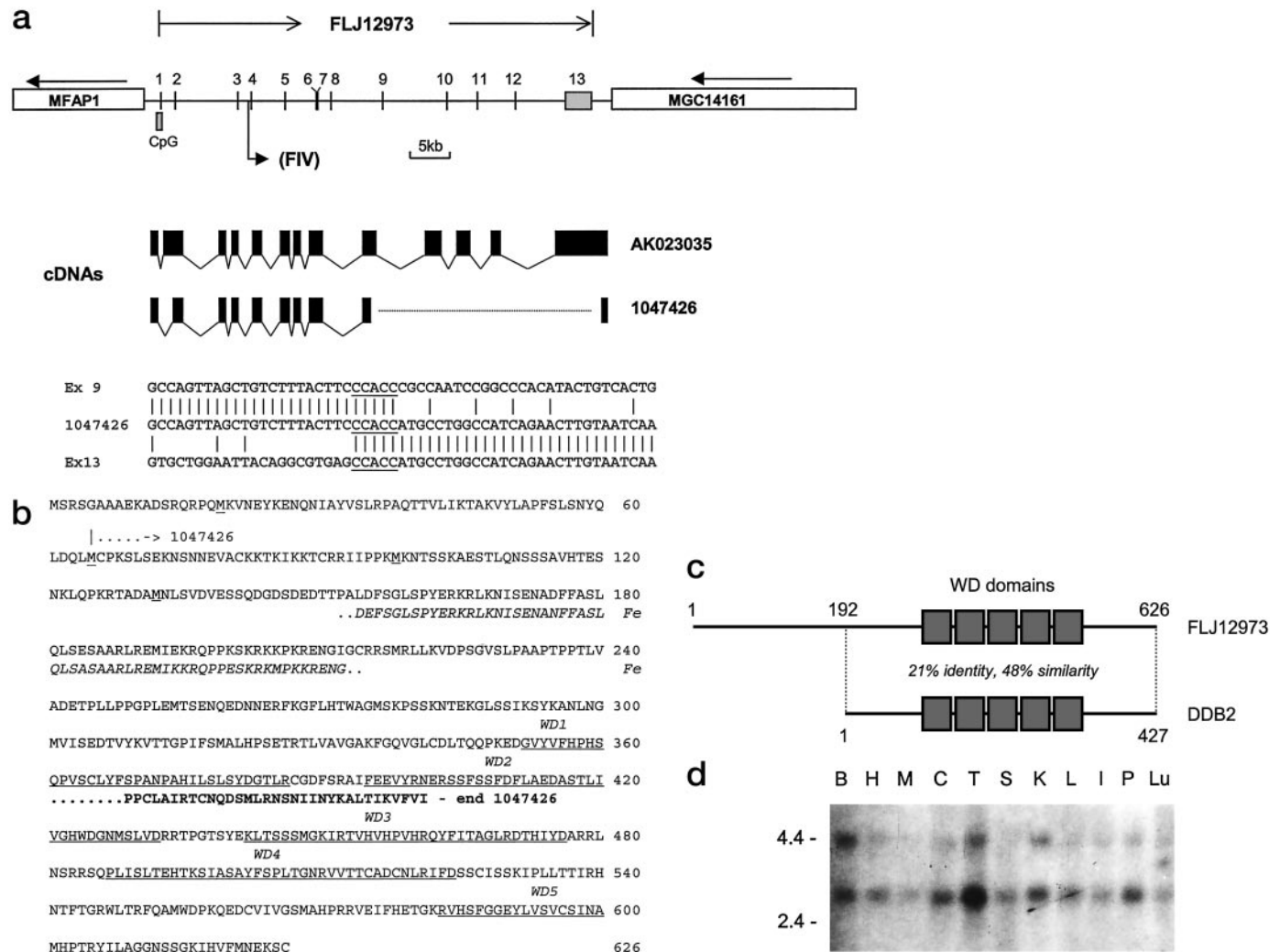


Fig. 2. *a*, Genomic structure of the human chromosome 15q15 surrounding the *FLJ12973* gene, based on the draft human genome sequence.⁷ Exons are indicated by numbered vertical lines and boxes along with the location of a CpG island at the 5' end of the gene. The relative position of the FIV insertion in the orthologous feline gene is indicated by an arrow. Adjacent genes in the opposite transcriptional orientation are indicated by open boxes. The structure of spliced EST and cDNA clones is shown below based on published sequence (AK023025) and our own analysis of an EST clone from the gene (IMAGE clone 1047426). Exon sizes are expanded for clarity. Clone 1047426 demonstrates alternative splicing in exon 2, and a deletion between exons 9 and 13. The sequences surrounding the intra-exon deletion are shown at the bottom of the figure, with a 5-bp region of homology underlined. *b*, predicted amino acid sequence of *FLJ12973*. The primary sequence illustrated here is the full-length 626 amino acid product predicted from cDNA AK023025. A number of other potential initiator methionines are underlined. The first potential initiator in the EST clone (IMAGE clone 1047426) is also indicated (*MCPKS*), and the frame-shifted COOH-terminal sequence of this clone is depicted underneath (*bold face*). The predicted amino acid sequence of the feline *FLJ12973* gene between exons 3 and 5 (Fe) is also shown in *italics* underneath. *c*, structural similarity between the predicted *FLJ12973* product and the human *DDB2* protein. Homology between these proteins is seen over the entire *DDB2* protein and the COOH-terminus of *FLJ12973*, and includes a series of five tandem WD40 repeats. *d*, expression of *FLJ12973* gene transcripts in normal human tissues. A multitissue blot obtained from a commercial supplier (Clontech) was preloaded with poly-A+ RNA from various tissue sources (B, brain; H, heart; M, skeletal muscle; C, colon; T, thymus; S, spleen; K, kidney; L, liver; I, intestine; P, placenta; Lu, lung). The blot was probed with the full-length 1.2 kb insert from the *FLJ12973* EST clone (IMAGE clone 1047426). The relative migration of size markers (4.4 and 2.4 kb) is indicated.

malian species (data not shown). As shown in Fig. 1c, feline-human sequence match is evident over the entire exon 3 of FLJ12973, which is coextensive with the feline exon apart from a single codon deletion. Homology extends 55 bp upstream and 9 bp downstream of the canonical splice acceptor and donor signals, which mark the exon boundaries (Fig. 1c). These observations unequivocally identify the feline orthologue of *FLJ12973* as the gene interrupted by proviral insertion at *FIVi-1* in lymphoma Q254.

The structure of the human *FLJ12973* gene in Fig. 2a, which is based on the annotated draft sequence, shows a gene comprising 13 exons and covering 40 kb of the human genome on chromosome 15q15. The first exon occurs within a CpG island, which also marks the boundary with the next 5' gene (*MFAP1*), which is in the opposite orientation. The relative position of FIV insertion in the orthologous feline gene is also indicated, which is between exons 3 and 4, in the same transcriptional orientation as the cellular gene. The exon structure of cDNAs derived from the human gene are indicated below, including the full-length transcript, which was derived from the NT2 teratocarcinoma cell line (AK023035). An interesting variation emerged from our analysis of an EST clone (IMAGE clone 1047426), which we obtained from the United Kingdom MRC HGMP Resource Centre (AA625226). Complete sequence analysis of this clone revealed a 1126-bp insert, which differed from the full-length transcript by an alternative splice in exon 2 and an internal deletion spanning from the middle of exon 9 to the extreme 3' end of exon 13. The deletion site is marked by a 5-bp homology (CCACC) between these exons (Fig. 2a), suggesting that this is not a normal splicing variant. Intriguingly, the same motif is repeated at the site of natural deletion variants of the *MECP2* gene, which is responsible for Rett syndrome, a progressive neurological disorder (14). As the EST clone came from the Soares library, which was generated from heterogenous RNA sources, the origins of this deletion are unclear, but the possible existence of natural variants of this gene clearly merits additional study.

The differences between the two FLJ12973 cDNA clones create ambiguity with respect to the predicted gene products as shown in Fig. 2b. The longest possible product is a 626 amino acid protein (MSRSG), whereas the alternatively spliced AA625226 cDNA clones suggests an alternative initiation (MCPKS). However, alignment with an EST from the orthologous murine gene (AK020004) shows that neither of these is conserved in the mouse. Use of the first conserved initiator codon would generate a 529 amino acid protein with the NH₂-terminal sequence MKNNTS. This sequence displays the closest match to the Kozak consensus (15). Clearly, additional direct analysis will be required to establish the true NH₂ terminus of FLJ12973 and its orthologues. The truncated cDNA AA625226 also encodes a frame-shift truncation with respect to the full-length gene product (Fig. 2b). Notably, the insertion site of FIV between exons 3 and 4 is 3' with respect to all of these potential translational initiation sites.

Analysis of FLJ12973 for known protein family domains revealed a series of five tandem WD40 repeats in a 250 amino acid COOH-terminal domain (Fig. 2, b and c). This protein-protein interaction motif is found in an expanding range of protein families of which the roles include transcriptional regulation, apoptosis induction, and signal transduction (16). Alignment with database sequences using the Smith and Waterman algorithm (MPSRCH)⁶ revealed that the closest human gene homologue is *DDB2*, the small subunit of a DNA damage-binding protein complex, which is defective in xeroderma pigmentosum patients of complementation group E (17). As shown in the diagram in Fig. 2c, the *DDB2* protein is remarkably similar to

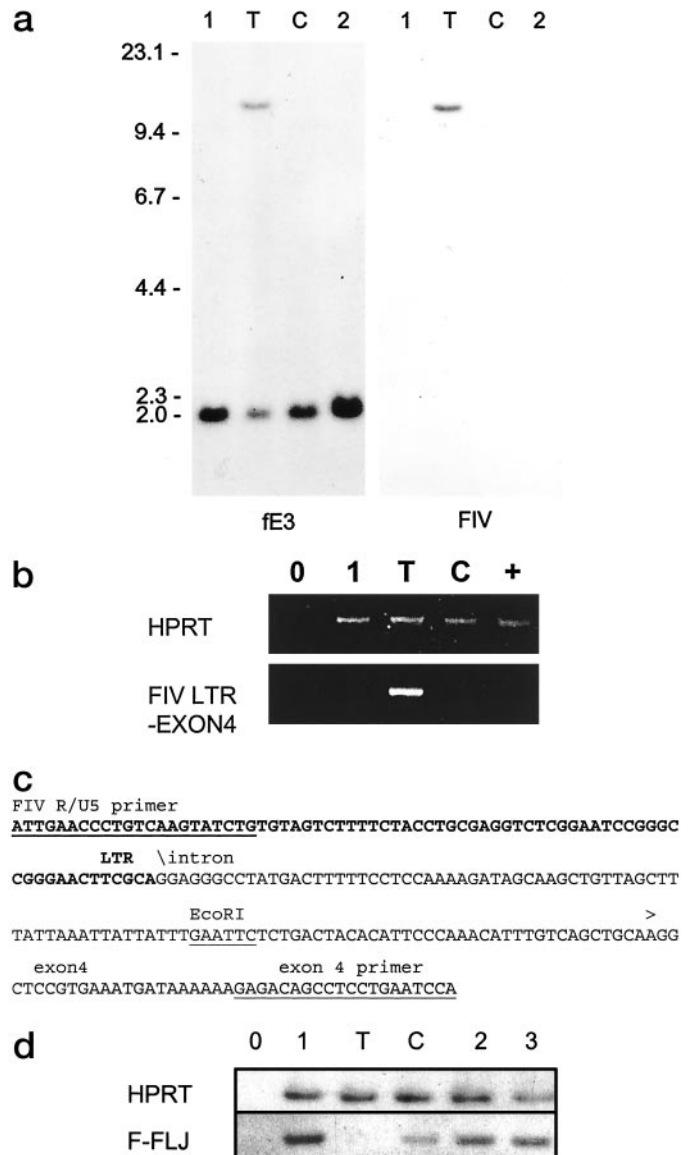


Fig. 3. *a*, Southern blot hybridization analysis was conducted using probe fE3 from the FIV integration site (Fig. 1a). This analysis shows the presence of a clonal rearrangement of the feline genome at the FIV insertion site in lymphoma Q254. The fragment size is consistent with the presence of an integrated FIV provirus in all cells of the tumor mass, whereas the lack of rearrangement in uninvolved tissue (salivary gland) from the same animal (C) excludes germ-line polymorphism as the basis of this phenomenon. Other control feline DNA samples were analyzed in Lanes 1 (AH927 fibroblast cells) and 2 (FL74 lymphoma cells). The right panel shows the results of reprobng the blot with an FIV-specific probe (*Gag-pol* and *Env*), which shows that the single FIV copy is coincident with the rearranged host gene fragment. *b*, detection of fusion transcripts in lymphoma Q254 by RT-PCR. Primers from the FIV LTR and F-FLJ12973 exon 4 were used to screen for fusion transcripts. The amplified products were separated on a polyacrylamide gel and detected by ethidium bromide staining. Samples include Q254 lymphoma (T), salivary gland (C). Control samples include no added RNA (0), feline fibroblast RNA (1), and the FIV-infected FL4 cell line (+). *c*, sequence of fusion transcripts derived from the FIV insertion site. DNA sequence determination of the transcript detected in *b* showed that this spans the 3' virus host junction. This structure suggests that the transcript may have arisen from activity of the 3' LTR promoter element. FIV LTR sequence is shown in bold. Also marked are the exon 4 splice acceptor site (>) and the *EcoRI* site, which marks the boundary of the cloned provirus (Fig. 1a). *d*, RT-PCR analysis of feline FLJ12973 (*F-FLJ*) expression. PCR was carried out using primers derived from exons 3 and 4 of the feline FLJ12973 orthologue (*F-FLJ*) or a control housekeeping gene (*HPRT*). The amplified products were separated on polyacrylamide gels, blotted and probed with a feline FLJ12973 probe (fE3) or *HPRT*. Samples analyzed in this way include Q254 lymphoma (T), salivary gland (C). Control samples include no added RNA (0), feline fibroblast RNA (1 and 3), or feline lymphoma F422 (2).

⁶ Internet address: <http://www.ebi.ac.uk>.

FLJ12973 in overall structure. It shares five tandem WD40 repeats and can be aligned with the COOH-terminal portion of FLJ12973 over its entire length with very few gaps.

The expression pattern of the human *FLJ12973* gene was explored by Northern blot analysis using a multitissue blot (Clontech; Fig. 2*d*). As can be seen from this analysis, the 1.2 kb EST probe (IMAGE clone 1047426) detected two transcripts—a major species at around 2.8 kb and a less abundant RNA of 4.5 kb. The smaller transcript is similar in size to that expected from the full-length cDNA sequence (AK023035), and a notable feature is the expression of FLJ12973 in all of the tissues examined. Expression levels varied very little across tissues, although some differences in relative abundance of the two transcripts were noted. Similarly, analyses of murine and feline tissue blots showed ubiquitous and relatively uniform patterns of expression, although in these cases only a single mRNA species was observed, with sizes of 4.5 kb and 3.5 kb, respectively (data not shown).

In the light of the foregoing observations, it was important to determine the effects of proviral insertion on the structure and expression of the feline *FLJ12973* gene. The use of an exon 3 (E3) probe for Southern blot analysis of a range of feline DNA samples (Fig. 3*a*) confirmed that the locus was clonally rearranged in lymphoma Q254, which displayed an *EcoRI* fragment of ~11.5 kb (R) corresponding precisely to the size predicted for the cloned provirus and its flanking sequences. A coincident fragment was detected with an FIV-specific probe (Fig. 3*a*, right panel). The 2-kb *EcoRI* fragment corresponding to the unoccupied *FIVi-1* site (U) was proportionately reduced in intensity in Q254 tumor DNA (T). Analysis of control tissue (C) from the same cat excluded the possibility of an inherited polymorphism at this locus. These results confirm that the FIV provirus was acquired somatically in lymphoma Q254 and indicate that insertion of this element at *FIVi-1* preceded clonal expansion of the lymphoma cells.

From the position of insertion within the gene (Fig. 2*a*), we considered it possible that a truncated or fused mRNA species might be generated. As discussed above, limited availability of primary tumor material constrained expression analysis. A single Northern blot was generated and analyzed with a probe spanning exons 3/4 of the feline gene, revealing no detectable signal in Q254 tumor RNA (data not shown). However, whereas this analysis ruled out gross overexpression, the low control hybridization signal meant that no conclusion could be drawn with regard to possible transcriptional down-regulation of the gene. Additional analysis by RT-PCR was undertaken to test for the presence of fusion transcripts initiating in viral sequences. As shown in Fig. 3*b*, primers spanning FIV LTR and exon 4 of F-FLJ12973 detected a transcript specifically in RNA derived from Q254 tumor cells, showing that read-through transcripts were indeed present, although presumably at low levels. Sequence analysis confirmed that these represented unspliced transcripts containing 3'LTR and host F-FLJ12973 intron 3 sequences (Fig. 3*c*). To test for the effect of insertion on the normal transcription pattern of F-FLJ12973, RT-PCR was also carried out using primers from exons 3 and 4. As can be seen in Fig. 3*d*, this assay readily detected transcripts in a range of feline cell lines (and other tissues; data not shown), with the exception of tumor Q254. The presence of transcripts in control tissue (salivary gland) from the same animal demonstrated that this evident loss of expression was not a constitutive defect.

Taken together, these results suggest that the consequence of FIV insertion in the feline *FLJ12973* gene may be loss of function. The status of the unaffected allele in the Q254 tumor cells is of interest in this respect. Southern blot analysis (Fig. 3*a*) shows a normal sized *EcoRI* fragment corresponding to the unaffected allele, showing that

at least part of the normal gene was retained in the tumor cell genome. The possibility that a deletion has occurred elsewhere in the gene cannot be excluded, whereas it is also conceivable that epigenetic silencing has occurred by a mechanism such as promoter hypermethylation, which can affect suppressor genes (18). In this respect it is interesting to note the close structural relationship of FLJ12973 to DDB2, one of the components of the xeroderma pigmentosum group E complex. DNA repair defects are commonly observed in lymphomas, and this class of gene has also been shown to be subject to epigenetic regulation (19). Such an event could conceivably mediate tumor initiation, particularly in the context of a B-cell population under proliferative stress, as seen in FIV infection (20). However, other loss-of-function effects potentially relevant to oncogenesis should not be discounted, as WD40 domain protein families execute many regulatory functions (21). The possibility of a wider role for FLJ12973 inactivation also merits additional study. Human chromosome 15q is the site of frequent deletions in ovarian (22) and sporadic colorectal cancers (23), whereas the latter tumor type is also associated with an inherited susceptibility gene, *CRAC1*, which maps to a similar location (24). It will clearly be important for future studies to characterize the *FLJ12973* gene in greater detail and to examine the biological consequences of functional inactivation.

This study reveals additional evidence of the direct mutagenic capacity of the immunosuppressive lentiviruses and their potential contribution as direct agents in carcinogenesis. The possibility of such a role has generally been ignored in recent analyses of AIDS-related malignancies. Our findings should rekindle interest in this field of study and raise awareness of the potential risks associated with lentivirus-based vectors, which are being developed currently for clinical use. It will be important to monitor the sites of integration of these agents *in vivo* and to examine their capacity to silence as well as activate host cell genes.

Acknowledgments

We thank Dr. Keith Vass for assistance with bioinformatics.

References

- Coffin, J. M., Hughes, S. H., and Varmus, H. E. *Retroviruses*. New York: Cold Spring Harbor Laboratory Press, 1997.
- Munroe, D. G., Peacock, J. W., and Benchimol, S. Inactivation of the cellular p53 gene is a common feature of Friend virus-induced erythroleukemia: relationship of inactivation to dominant transforming activity. *Mol. Cell Biol.*, 10: 3307–3313, 1990.
- Hernandez, A. M., and Shibata, D. Epstein-Barr virus-associated non-Hodgkin's lymphoma in HIV-infected patients. *Leuk. Lymphoma*, 16: 217–221, 1995.
- Beatty, J. A., Lawrence, C. E., Callanan, J. J., Grant, C. K., Gault, E. A., Neil, J. C., and Jarrett, O. Feline immunodeficiency virus (FIV)-associated lymphoma: a potential role for immune dysfunction in tumorigenesis. *Vet. Immunol. Immunopathol.*, 65: 309–322, 1998.
- Terry, A., Callanan, J. J., Fulton, R., Jarrett, O., and Neil, J. C. Molecular analysis of feline immunodeficiency virus-associated tumours: an indirect role for FIV. *Int. J. Cancer*, 61: 1–6, 1995.
- Shiramizu, B., Herndier, B. G., and McGrath, M. S. Identification of a common clonal human immunodeficiency virus integration site in human immunodeficiency virus-associated lymphomas. *Cancer Res.*, 54: 2069–2072, 1994.
- McGrath, M. S., Shiramizu, B. T., and Herndier, B. G. Identification of a clonal form of HIV in early Kaposi's sarcoma: evidence for a novel model of oncogenesis, "sequential neoplasia". *J. Acquir. Immune. Defic. Syndr.*, 8: 379–385, 1995.
- Herndier, B. G., Shiramizu, B. T., Jewett, N. E., Aldape, K. D., Reyes, G. R., and McGrath, M. S. Acquired immunodeficiency syndrome-associated T-cell lymphoma: evidence for human immunodeficiency virus type I-associated T-cell transformation. *Blood*, 79: 1768–1774, 1992.
- Beatty, J. A., Callanan, J. J., Terry, A., Jarrett, O., and Neil, J. C. Molecular and immunophenotypic characterisation of a feline immunodeficiency virus (FIV)-associated lymphoma: A direct role for FIV in B-lymphocyte transformation? *J. Virol.*, 72: 767–771, 1998.
- Rigby, M. A., Holmes, E. C., Pistello, M., Mackay, A., Leigh Brown, A. J., and Neil, J. C. Evolution of structural proteins of feline immunodeficiency virus: molecular epidemiology and evidence of selection for change. *J. Gen. Virol.*, 74: 425–436, 1993.
- O'Brien, S. J., Seuanez, H. N., and Womack, J. E. Mammalian genome organization: an evolutionary view. *Annu. Rev. Genet.*, 22: 323–351, 1988.

⁷ Internet address: <http://genome.ucsc.edu>.

12. Rigby, M. A., Hosie, M. J., Willett, B. J., Mackay, N., McDonald, M., Cannon, C., Dunsford, T., Jarrett, O., and Neil, J. C. Comparative efficiency of feline immunodeficiency virus infection by DNA inoculation. *AIDS Res. Hum. Retrovir.*, *13*: 403–410, 1997.
13. Wienberg, J., Stanyon, R., Nash, W. G., O'Brien, P. C., Yang, F., O'Brien, S. J., and Ferguson-Smith, M. A. Conservation of human vs. feline genome organization revealed by reciprocal chromosome painting. *Cytogenet. Cell Genet.*, *77*: 211–217, 1997.
14. Bienvenu, T., Carrie, A., de Roux, N., Vinet, M. C., Jonveaux, P., Couvert, P., Villard, L., Arzimanoglou, A., Beldjord, C., Fontes, M., Tardieu, M., and Chelly, J. MECP2 mutations account for most cases of typical forms of Rett syndrome. *Hum. Mol. Genet.*, *9*: 1377–1384, 2000.
15. Kozak, M. Comparison of initiation of protein synthesis in prokaryotes, eukaryotes, and organelles. *Microbiol. Rev.*, *47*: 1–45, 1983.
16. Li, D., and Roberts, R. WD-repeat proteins: structure characteristics, biological function, and their involvement in human diseases. *Cell Mol. Life Sci.*, *58*: 2085–2097, 2001.
17. Dualan, R., Brody, T., Keeney, S., Nichols, A. F., Admon, A., and Linn, S. Chromosomal localization and cDNA cloning of the genes (DDB1 and DDB2) for the p127 and p48 subunits of a human damage-specific DNA binding protein. *Genomics*, *29*: 62–69, 1995.
18. Herman, J. G., and Baylin, S. B. Promoter-region hypermethylation and gene silencing in human cancer. *Curr. Top. Microbiol. Immunol.*, *249*: 35–54, 2000.
19. Esteller, M., Gaidano, G., Goodman, S. N., Zagonel, V., Capello, D., Botto, B., Rossi, D., Ghoghini, A., Vitolo, U., Carbone, A., Baylin, S. B., and Herman, J. G. Hypermethylation of the DNA repair gene o(6)-methylguanine DNA methyltransferase and survival of patients with diffuse large B-cell lymphoma. *J. Natl. Cancer Inst.*, *94*: 26–32, 2002.
20. Flynn, J. N., Cannon, C. A., Lawrence, C. E., and Jarrett, O. Polyclonal B-cell activation in cats infected with feline immunodeficiency virus. *Immunology*, *81*: 626–630, 1994.
21. Apidianakis, Y., Grbavec, D., Stifani, S., and Delidakis, C. Groucho mediates a Ci-independent mechanism of hedgehog repression in the anterior wing pouch. *Development (Camb.)*, *128*: 4361–4370, 2001.
22. Zweemer, R. P., Ryan, A., Snijders, A. M., Hermsen, M. A., Meijer, G. A., Beller, U., Menko, F. H., Jacobs, I. J., Baak, J. P., Verheijen, R. H., Kenemans, P., and van Diest, P. J. Comparative genomic hybridization of microdissected familial ovarian carcinoma: two deleted regions on chromosome 15q not previously identified in sporadic ovarian carcinoma. *Lab. Investig.*, *81*: 1363–1370, 2001.
23. Park, W. S., Park, J. Y., Oh, R. R., Yoo, N. J., Lee, S. H., Shin, M. S., Lee, H. K., Han, S., Yoon, S. K., Kim, S. Y., Choi, C., Kim, P. J., Oh, S. T., and Lee, J. Y. A distinct tumor suppressor gene locus on chromosome 15q21.1 in sporadic form of colorectal cancer. *Cancer Res.*, *60*: 70–73, 2000.
24. Tomlinson, I., Rahman, N., Frayling, I., Mangion, J., Barfoot, R., Hamoudi, R., Seal, S., Northover, J., Thomas, H. J., Neale, K., Hodgson, S., Talbot, I., Houlston, R., and Stratton, M. R. Inherited susceptibility to colorectal adenomas and carcinomas: evidence for a new predisposition gene on 15q14–q22. *Gastroenterology*, *116*: 789–795, 1999.

Cancer Research

The Journal of Cancer Research (1916–1930) | The American Journal of Cancer (1931–1940)

Feline Immunodeficiency Virus Integration in B-Cell Lymphoma Identifies a Candidate Tumor Suppressor Gene on Human Chromosome 15q15

Julia Beatty, Anne Terry, Julie MacDonald, et al.

Cancer Res 2002;62:7175-7180.

Updated version Access the most recent version of this article at:
<http://cancerres.aacrjournals.org/content/62/24/7175>

Cited articles This article cites 22 articles, 7 of which you can access for free at:
<http://cancerres.aacrjournals.org/content/62/24/7175.full#ref-list-1>

Citing articles This article has been cited by 1 HighWire-hosted articles. Access the articles at:
<http://cancerres.aacrjournals.org/content/62/24/7175.full#related-urls>

E-mail alerts [Sign up to receive free email-alerts](#) related to this article or journal.

Reprints and Subscriptions To order reprints of this article or to subscribe to the journal, contact the AACR Publications Department at pubs@aacr.org.

Permissions To request permission to re-use all or part of this article, use this link
<http://cancerres.aacrjournals.org/content/62/24/7175>.
Click on "Request Permissions" which will take you to the Copyright Clearance Center's (CCC) Rightslink site.